Chemistry & Biology
Article

Biosynthesis of Rhizocticins, Antifungal Phosphonate Oligopeptides Produced by *Bacillus subtilis* ATCC6633

Svetlana A. Borisova,[1] Benjamin T. Circello,[1,2] Jun Kai Zhang,[2] Wilfred A. van der Donk,[1,3,4,*] and William W. Metcalf[1,2,*]
[1]Institute for Genomic Biology
[2]Department of Microbiology
[3]Department of Chemistry
[4]Howard Hughes Medical Institute
University of Illinois at Urbana-Champaign, Urbana, IL 61801, USA
*Correspondence: vddonk@uiuc.edu (W.A.V.), metcalf@uiuc.edu (W.W.M.)
DOI 10.1016/j.chembiol.2009.11.017

SUMMARY

Rhizocticins are phosphonate oligopeptide antibiotics containing the C-terminal nonproteinogenic amino acid (*Z*)-L-2-amino-5-phosphono-3-pentenoic acid (APPA). Here we report the identification and characterization of the rhizocticin biosynthetic gene cluster (*rhi*) in *Bacillus subtilis* ATCC6633. Rhizocticin B was heterologously produced in the nonproducer strain *Bacillus subtilis* 168. A biosynthetic pathway is proposed on the basis of bioinformatics analysis of the *rhi* genes. One of the steps during the biosynthesis of APPA is an unusual aldol reaction between phosphonoacetaldehyde and oxaloacetate catalyzed by an aldolase homolog RhiG. Recombinant RhiG was prepared, and the product of an in vitro enzymatic conversion was characterized. Access to this intermediate allows for biochemical characterization of subsequent steps in the pathway.

INTRODUCTION

Rhizocticins are phosphonate-containing oligopeptide antibiotics produced by the gram-positive bacterium *B. subtilis* ATCC6633. They were originally discovered in 1949 on the basis of their antifungal activity and were collectively termed "rhizoctonia factor" (Michener and Snell, 1949). The structures of rhizocticins were determined 40 years later (Rapp et al., 1988). They are di- and tripeptide antibiotics consisting of a variable amino acid at the N terminus followed by arginine and the nonproteinogenic amino acid (*Z*)-L-2-amino-5-phosphono-3-pentenoic acid (APPA; Figure 1A). Interestingly, APPA is also the C-terminal amino acid of the tripeptide antibiotics plumbemycin A and B produced by *Streptomyces plumbeus* (Figure 1B) (Park et al., 1977a; Park et al., 1977b).

Rhizocticins enter the target fungal cell through the oligopeptide transport system (Kugler et al., 1990). They are then cleaved by host peptidases to release APPA, which inhibits threonine synthase, an enzyme catalyzing the pyridoxal 5′-phosphate (PLP)–dependent conversion of phosphohomoserine to L-threonine (Figure 1C) (Kugler et al., 1990; Laber et al., 1994). Hence, APPA interferes with the biosynthesis of threonine and related metabolic pathways, ultimately affecting protein synthesis and leading to growth inhibition. The inhibitory activity of APPA is due to the structural resemblance to phosphohomoserine, but it possesses a hydrolytically stable C-P bond in place of the C-O-P moiety of phosphohomoserine.

Rhizocticins exhibit antifungal activity, whereas plumbemycins are antibacterials. It has been demonstrated that plumbemycins also enter *Escherichia coli* K-12 via the oligopeptide transport system (Diddens et al., 1979). As in the case of rhizocticins, L-threonine reverses the growth inhibition by plumbemycins in a concentration-dependent manner (Park et al., 1977b). Therefore, similarly to rhizocticins, plumbemycins must be cleaved by peptidases of the target cell to release the active substance, APPA. The selectivity of these tripeptide antibiotics is thus not due to a difference in mode of action, but rather is determined by the recognition of proteinogenic amino acids attached at the N terminus of APPA by a specific oligopeptide transport system or peptidase. This feature can potentially be exploited to create APPA-containing oligopeptides with specific selectivity for a particular organism. Furthermore, the target of APPA, threonine synthase, is not present in mammals, reducing the likelihood of toxicity to humans. Thus, such phosphonate oligopeptides can be promising therapeutics.

Phosphonate compounds are prevalent among biologically active molecules, mainly because of their ability to function as stable mimics of carboxylate and phosphate-containing metabolites. At present, biosynthetic pathways of only a handful of phosphonates have been extensively studied (see Metcalf and van der Donk, 2009 for a recent comprehensive review on the topic), including fosfomycin (Hidaka et al., 1995; Woodyer et al., 2006), dehydrophos (B. T. Circello and W.W.M., unpublished data), FR-900098 (Eliot et al., 2008), and phosphinothricin-containing peptides (e.g., PTT) (Blodgett et al., 2007) (Figure 1D). These studies have shown that the biosyntheses of this class of compounds provide a rich source of novel biochemistry as exemplified by many unique enzymatic transformations (Cicchillo et al., 2009; Higgins et al., 2005). Therefore, a better understanding of the rhizocticin pathway will be of great interest. Furthermore, biosynthetic access to the APPA warhead of the rhizocticins would be advantageous because organic

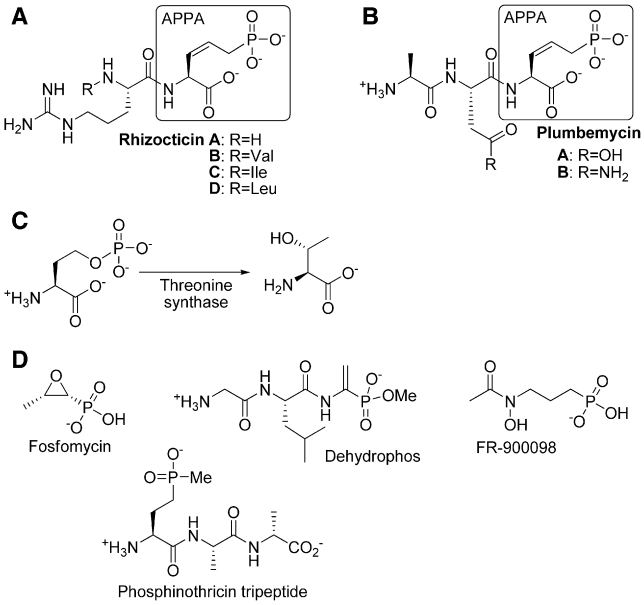

Figure 1. Chemical Structures of the Phosphonate Antibiotics

(A) Chemical structure of rhizocticins.

(B) Chemical structure of plumbemycins.

(C) The threonine synthase reaction inhibited by APPA.

(D) Chemical structures of representative phosphonate antibiotics whose biosynthetic pathways have been studied.

synthesis of this molecule is very challenging. For instance, biosynthetic preparation of APPA would provide an avenue to combinatorially vary the N-terminal amino acids to create analogs with desired specificity.

To this end, we identified the rhizocticin biosynthetic cluster in the genome of *B. subtilis* ATCC6633 and confirmed its identity by heterologous expression in *B. subtilis* 168. Although the first two steps of the biosynthetic pathway appear to be the same as for other phosphonate metabolites, the third step—an aldol reaction between phosphonoacetaldehyde (PnAA) and oxaloacetic acid (OAA)—is unprecedented. Biochemical characterization of this step is also reported here. On the basis of genetic and biochemical information, a pathway for the biosynthesis of rhizocticins is proposed.

RESULTS AND DISCUSSION

Identification of the Rhizocticin Biosynthetic Gene Cluster

The first step in the biosynthetic pathways of the majority of phosphonates is the isomerization of phosphoenolpyruvate (PEP) to phosphonopyruvate (PnPy) catalyzed by phosphoenolpyruvate phosphomutase (PEP mutase) (Seidel et al., 1988). Previously, we successfully identified phosphonate biosynthetic gene clusters by screening fosmid libraries with degenerate PCR primers designed to amplify PEP mutase-encoding genes (Blodgett et al., 2005; Eliot et al., 2008). We attempted a similar approach here to identify the rhizocticin gene cluster. A fosmid library of *B. subtilis* ATCC6633 was constructed and screened by PCR for a PEP mutase gene fragment as described in the Supplemental Information available online. However, none of

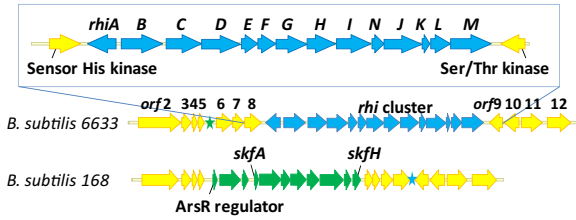

Figure 2. Organization of the Rhizocticin Gene Cluster and Surrounding Genes on the *B. subtilis* ATCC6633 Chromosome

The same locus of *B. subtilis* 168 genome is also shown for comparison. Genes with a high degree of homology between the two strains (>90% identity) are shown in yellow. The biosynthetic clusters for rhizocticin and sporulation killing factor are shown in blue and green, respectively. The corresponding location of these loci in the other genome is denoted with a star of the same color.

the clones produced the desired PCR fragment, possibly because of a highly divergent sequence of the PEP mutase gene, which prevented annealing of the primers. Alternatively, a PEP mutase–independent pathway might be used by *B. subtilis* ATCC6633 for production of rhizocticin.

To investigate these alternatives, the genome of *B. subtilis* ATCC6633 was sequenced using the 454 sequencing platform. The details of the genome sequencing will be reported elsewhere. Briefly, sequencing data were assembled into 37 contigs spanning approximately 4.0 Mb. A total of 3769 open reading frames (ORFs) were determined and annotated using the RAST Server (Rapid Annotations using Subsystems Technology) (Aziz et al., 2008). For comparison, the closely related *B. subtilis* 168 strain has a genome of 4.2 Mb comprising 4114 coding sequences (Kunst et al., 1997). When searched for the PEP mutase gene, the sequence of the genome of *B. subtilis* ATCC6633 produced a single hit. This gene appears to be a part of an operon consisting of 13 ORFs and is preceded by a differentially transcribed additional ORF encoding a transcriptional regulator. Careful analysis of the ORFs comprising this operon led to the conclusion that these genes are likely to constitute a rhizocticin biosynthetic gene cluster (Figure 2).

With the genome sequence available, the fosmid library of *B. subtilis* ATCC6633 was screened as described above using two sets of sequence-specific primers designed to amplify short sequences upstream of the putative rhizocticin cluster (within *orf6*) and within *rhiM*. Fosmid 2-11E was identified and sequenced via the Sanger protocol using transposon insertions, as described elsewhere (Blodgett et al., 2005; Eliot et al., 2008). The sequence of the insert of 2-11E originating from *B. subtilis* ATCC6633 DNA was identical to that of the corresponding fragment obtained through 454 sequencing of the genome, with the exception of a single base-pair mismatch located outside of the putative rhizocticin gene cluster.

B. subtilis ATCC6633 possesses a high degree of nucleotide sequence homology to *B. subtilis* 168. The putative rhizocticin gene cluster appears to be a single site insertion of approximately 13 kb into the genome of *B. subtilis* 168. Although the genes of the rhizocticin cluster have no homologs within the *B. subtilis* 168 genome, the nucleotide sequences outside of the cluster are approximately 90% identical. Interestingly, *B. subtilis* 168 contains a gene cluster (*skf*) located near the "insertion site" of the rhizocticin gene cluster (blue star in

Table 1. Summary of the Open Reading Frames of the Rhizocticin Gene Cluster

ORF	No. of aa	Protein homology (NCBI No.)	Percentage of aa identity[a]
orf6	325	*B. subtilis* 168 putative hydrolase/transferase (CAB11993) (325 aa)	94
orf7	223	*B. subtilis* 168 two-component response regulator YbdJ (BAA33098) (223 aa)	95
orf8	322	*B. subtilis* 168 sensor histidine kinase YbdK (BAA33099) (320 aa)	87
rhiA	296	*B. licheniformis* transcriptional activator of the *cysJI* operon (AAU21843) (298 aa)	65
		Salmonella enterica Typhimurium transcriptional regulator CysB (NP_460672) (324 aa)	18
rhiB	433	*Sphaerobacter thermophilus* threonine synthase (ZP_04494878) (420 aa)	46
		Mycobacterium tuberculosis threonine synthase (2D1F_B) (360 aa)	28
		B. subtilis ATCC6633 threonine synthase ThrC (this study) (352 aa)	27
rhiC	408	*B. licheniformis* hypothetical protein, related to NikS (YP_077482) (405 aa)	62
		Streptomyces ansochromogenes nikkomycin biosynthesis protein SanS, D-Ala-D-Ala ligase homolog (AAK53061) (424 aa)	30
rhiD	407	*B. licheniformis* MFS transporter (YP_077483) (408 aa)	68
rhiE	167	*Sorangium cellulosum* sulfopyruvate decarboxylase α-subunit (YP_001617955) (170 aa)	40
rhiF	186	*S. hygroscopicus* phosphonopyruvate decarboxylase (Q54271) (401 aa)	40
rhiG	337	*Legionella pneumophila* 4-hydroxy-2-oxovalerate aldolase (YP_096686) (295 aa)	34
		Pseudomonas sp. bifunctional aldolase-dehydrogenase DmpG (1NVM_A) (345 aa)	25
rhiH	296	*Paenibacillus larvae* putative PEP phosphomutase (ZP_02329666) (297 aa)	56
		S. viridochromogenes PEP phosphomutase of PTT biosynthesis (AAU00071) (313 aa)	42
rhiI	362	*Pseudomonas syringae* hypothetical protein (BAF32889) (354 aa)	36
		Mycoplasma pneumonia HPr kinase/phosphatase (1KNX_A) (312 aa)	14
rhiN	132	*Chloroherpeton thalassium* protein of unknown function UPF0047 (YP_001997537) (138 aa)	35
		E. coli conserved hypothetical protein YjbQ (ZP_03048862) (138 aa)	22
rhiJ	393	*Thermotoga lettingae* aminotransferase class V (YP_001471385) (381 aa)	42
		Methanocaldococcus jannaschii broad-specificity class V aspartate aminotransferase (NP_247954) (385 aa)	38
rhiK	85	*Natronomonas pharaonis* glutaredoxin (CAI48716) (82 aa)	35
		E. coli glutaredoxin 3 (1FOV_A) (82 aa)	23
rhiL	215	*Frankia* sp. EAN1pec putative metallophosphoesterase (YP_001510901) (243 aa)	32
		E. coli metal-dependent phosphodiesterase YfcE (P67095) (184 aa)	19
rhiM	413	*B. licheniformis* hypothetical, related to NikS (YP_077482) (405 aa)	25
		S. ansochromogenes nikkomycin biosynthesis protein SanS, D-Ala-D-Ala ligase homolog (AAK53061) (424 aa)	26
orf9	256	*B. subtilis* 168 putative serine/threonine protein kinase YbdM (O31435) (256 aa)	90
orf10	284	*B. subtilis* 168 putative phage protein YbdN (CAB11998) (285 aa)	94
orf11	394	*B. subtilis* 168 putative phage protein YbdO (CAB11999) (394 aa)	89

Note: aa, amino acid.
[a] The closest homologs were based on NCBI searches conducted October 8, 2009. The homolog whose biochemical function was experimentally supported is shown for proteins of particular interest.

Figure 2). This gene cluster is absent from *B. subtilis* ATCC6633 (its corresponding location is shown as a green star). The *skf* gene cluster is responsible for the biosynthesis and export of and the immunity to sporulation killing factor. This peptide antibiotic produced by sporulating *B. subtilis* 168 causes lysis of nonsporulating sibling *B. subtilis* 168 cells (Gonzalez-Pastor et al., 2003). Thus, the *rhi* and *skf* gene clusters occupy essentially the same locus on the genomic DNA of related species, as commonly seen for the genes involved in secondary metabolism.

Bioinformatic Analysis of the *rhi* Cluster

The genes of the rhizocticin biosynthetic cluster were first annotated using the RAST Server (Aziz et al., 2008) and further analyzed with the Basic Local Alignment Search Tool (BLAST) program at NCBI (Altschul et al., 1990) and the Phyre server (Kelley and Sternberg, 2009). The gene annotations, along with the closest and functionally confirmed homologs, are shown in Table 1.

As mentioned above, the genes surrounding the putative rhizocticin gene cluster (*rhiA-rhiM*; e.g., immediately adjacent *orf6-8* and *orf9-11*) have nearly identical counterparts in *B. subtilis* 168. Therefore, they are not likely to be involved in rhizocticin biosynthesis.

The *rhiA* gene encodes a putative transcriptional regulator of the LysR family (Schell, 1993). The helix-turn-helix DNA-binding motif, typical of many LysR regulators (Maddocks and Oyston, 2008), is predicted by the Phyre server to be located within the

N-terminal residues 30–85. A putative ligand-binding domain is also present at the C terminus of RhiA. The *rhiA* gene is located upstream and in the opposite direction of the other genes in the *rhi* operon, as commonly seen for LysR-regulated operons (Maddocks and Oyston, 2008).

The *rhiB* gene encodes a putative threonine synthase. Interestingly, the genome of *B. subtilis* ATCC6633 contains another copy of a threonine synthase gene, *thrC*, located in an operon with genes involved in the biosynthesis of threonine that is present at the same site as the threonine synthase gene in the *B. subtilis* 168 genome. Unlike RhiB, ThrC is highly homologous to threonine synthases of gram-positive bacteria, predominantly *Bacillus* species (98% identical to threonine synthase of *B. subtilis* 168), suggesting ThrC is a bona fide threonine synthase involved in primary metabolism. RhiB and ThrC appear to be evolutionary distinct because they share only 27% amino acid identity. It is conceivable that *rhiB* is involved in rhizocticin self-resistance by encoding a threonine synthase homolog that is not inhibited by APPA.

The translated products of *rhiC* and *rhiM* are homologs (26% identity). The proteins with the closest homology are NikS and SanS, participating in the biosynthesis of the peptidyl nucleoside antibiotic nikkomycin (Lauer et al., 2001; Li et al., 2004). They belong to the carboxylate-amine/thiol ligase superfamily of enzymes possessing a signature ATP-grasp structural motif (Galperin and Koonin, 1997). The enzymes of this superfamily catalyze the ATP-dependent formation of peptide or thioester bonds via a reactive acylphosphate intermediate. Examples include D-Ala-D-Ala ligase of peptidoglycan biosynthesis (Fan et al., 1994; Zawadzke et al., 1991), glutathione synthetase (Fan et al., 1995; Yamaguchi et al., 1993), and biotin carboxylase (Artymiuk et al., 1996; Waldrop et al., 1994). Despite a variety of reactions catalyzed by the members of the ATP-grasp superfamily, enzymes catalyzing the formation of a "conventional" proteinogenic α-peptide bond between L-amino acids have been identified only recently (Kino et al., 2009; Kino et al., 2008a; Kino et al., 2008b; Tabata et al., 2005). During the course of our study, the identification and substrate specificity of RhiM was reported (named RizA by the authors) (Kino et al., 2009). RhiM (RizA) is capable of ligating L-arginine to 19 other amino acids, including a saturated analog of L-APPA, 2-amino-5-phosphonopentanoic acid (Kino et al., 2009). A sequence of RhiC has also been deposited into GenBank (accession number BAH56723) by Kino and co-workers; its activity has not been reported.

RhiD is a putative transporter of the major facilitator superfamily (MFS). Between 8 and 10 transmembrane helixes are predicted by different topology prediction tools (http://ca.expasy.org). RhiD is likely responsible for the export of rhizocticins from the cell.

The genes *rhiE* and *rhiF* encode two subunits of a putative PnPy decarboxylase. PnPy decarboxylases catalyze the irreversible thiamin pyrophosphate (TPP)–dependent decarboxylation of PnPy to PnAA. This step is present in the majority of biosynthetic pathways of known phosphonates, including fosfomycin and phosphinothricin tripeptide (Metcalf and van der Donk, 2009). Unlike RhiE/RhiF, these enzymes usually consist of a single polypeptide chain. On the other hand, the functionally similar sulfopyruvate decarboxylase of coenzyme M biosynthesis is usually a two-subunit enzyme (e.g., ComD and ComE in *Methanococcus jannaschii*) (Graupner et al., 2000). ComD (α-subunit) is homologous to the N-terminal portion of single chain PnPy decarboxylases, whereas ComE (β-subunit) has homology to the C terminus. In a similar manner, RhiE and RhiF are homologs of the α- and β-subunits of sulfopyruvate decarboxylase, respectively, and the N- and C-terminal portions of single chain PnPy decarboxylases. RhiF (like ComE) contains a canonical TPP-binding motif. To the extent of our knowledge, RhiE/RhiF is the first example of a PnPy decarboxylase consisting of two subunits.

A search of the NCBI database for protein sequences homologous to the translated product of *rhiG* yielded a number of putative 4-hydroxy-2-oxovalerate aldolases with modest homology to RhiG (identity of 35% and lower). The closest homologs of RhiG that have been biochemically characterized are the 4-hydroxy-2-oxovalerate aldolases NahM and DmpG (25% identity) of *Pseudomonas putida* strains (Manjasetty et al., 2003; Platt et al., 1995). They belong to the class II family of aldolases that are dependent on divalent metal ions for catalysis. DmpG (and NahM) catalyzes the penultimate step of the *meta*-cleavage pathway from catechol to pyruvate and acetyl-CoA during the catabolism of aromatic compounds by *Pseudomonas* strains. DmpG is a part of a bifunctional enzyme complex because it physically associates with the enzyme of the following step, acetaldehyde dehydrogenase (acylating) DmpF, to ensure efficient transfer of the reactive intermediate acetaldehyde (Figure S1).

The *rhiH* gene encodes a putative PEP mutase that presumably would catalyze the first step in the biosynthetic pathway, the conversion of PEP to PnPy.

The translated product of *rhiI* has no significant end-to-end homology to any of the entries in the NCBI database. However, the C terminus of RhiI (approximately 213 amino acids) shows low homology to the C-terminal domain of the histidine-containing phospho carrier protein (HPr) kinase/phosphorylase from several species. In low GC gram-positive bacteria, HPr is involved in the regulation of carbon catabolism (Martin-Verstraete et al., 1999). HPr kinase/phosphorylase is a bifunctional protein that modifies Ser-46 of HPr and accepts ATP or pyrophosphate (PP_i) as a phosphate group donor. RhiI contains an easily identifiable canonical nucleotide binding P loop (**G**SK**G**K**GKS**). It is conceivable that RhiI catalyzes an ATP-dependent phosphorylation of a small molecule or plays a regulatory role similar to HPr kinase/phosphorylase.

The translated gene product of *rhiN* shows homology to a number of hypothetical proteins belonging to an uncharacterized protein family UPF0047 (ExPASy, Prosite). The members of this family are small proteins of 14–16 kDa and are widely distributed among the three domains of life. Although several crystal structures were solved (submitted to the Protein Data Bank but not published) for the UPF0047 family, no function has been established for any of the homologs. One of the UPF0047 proteins, YjbQ of *E. coli*, has a low promiscuous activity as thiamine phosphate synthase (Morett et al., 2008), catalyzing the coupling of the thiazole and pyrimidine portions of thiamine phosphate via a nucleophilic substitution reaction proceeding through a carbocation intermediate (Peapus et al., 2001). However, the biological function of YjbQ and its homologs remains to be elucidated.

The gene *rhiJ* encodes a putative aminotransferase belonging to a family of Fold Type I PLP-dependent enzymes (Eliot and Kirsch, 2004). It can be further classified into phylogenetic class V of aminotransferases (also referred to as subgroup IV) (Mehta et al., 1993). One of the closest homologs (38% identical) of RhiJ, MJ0959 of *Methanocaldococcus jannaschii*, displayed the highest specific activity for transamination of aspartate and α-ketoglutarate when assayed in vitro (Helgadottir et al., 2007). However, MJ0959 is thought to be a part of L-phosphoserine biosynthesis, converting phosphohydroxypyruvate to L-phosphoserine (Helgadottir et al., 2007).

BLAST analysis revealed that RhiK is a homolog of glutaredoxins, small proteins related to thioredoxins and involved in the maintenance of the reducing environment of the cytoplasm. RhiK contains a CPYC motif conserved among glutaredoxins and is predicted to have a typical βαβαββα thioredoxin fold (Pan and Bardwell, 2006). RhiK also shows homology to the N-terminal domain of glutathione *S*-transferase, another member of the thioredoxin-like superfamily.

The translated sequence of *rhiL* belongs to the calcineurin-like superfamily (PF00149) that includes metal-dependent phosphomonoesterases and phosphodiesterases catalyzing the hydrolysis of diverse substrates, from phosphorylated proteins to nucleic acids (Koonin, 1994). Several conserved amino acid residues are present in RhiL, most notably all those comprising the binuclear metal center, suggesting it may have a phosphodiesterase activity as well.

Heterologous Production of Rhizocticin B

To confirm that the identified gene cluster is responsible for the biosynthesis of rhizocticins in *B. subtilis* ATCC6633, we introduced the *rhi* cluster in the *B. subtilis* 168 genome through homologous recombination (see the Experimental Procedures and Figure S2 for details). To do this, a spectinomycin resistance cassette (Spec) was introduced into fosmid 2-11E downstream of the *rhi* cluster using λ Red recombinase-mediated recombination (Datsenko and Wanner, 2000). The resulting fosmid 2-11E+Spec was linearized by restriction digestion and used for the transformation of *B. subtilis* 168. We anticipated that the level of homology between the DNA sequence immediately outside of the *rhi* cluster in *B. subtilis* ATCC6633 and the corresponding sequence of *B. subtilis* 168 (over 90% identity on the nucleotide level) was sufficiently high for the homologous recombination to occur. This proved correct, because the recombinant *B. subtilis* 168 colonies selected on spectinomycin-containing medium contained the *rhi* cluster, as verified by PCR amplification of *rhiC* and *rhiM* genes.

One of the recombinant strains, *B. subtilis* MMG272, was grown for the production of rhizocticins, and its clarified spent medium was partially purified and fractionated as described in Experimental Procedures. Samples were analyzed by phosphorus (^{31}P) NMR spectroscopy for the presence of phosphonates. One of the fractions produced a major phosphonate peak with a characteristic chemical shift (δ) of 20.7 ppm in the ^{31}P NMR spectrum (Figure 3A). Addition of purified rhizocticin B to the sample resulted in an increase in intensity of the 20.7 ppm peak and no new peaks in the ^{31}P NMR spectrum (Figure 3A), suggesting that the major phosphonate product is rhizocticin B. Analysis of the sample by liquid chromatography-mass spectrometry (LC-MS) further supported the presence of rhizocticin B (see Figure 3B and Experimental Procedures for details). No phosphonates were produced in a control experiment with the parent *B. subtilis* 168 strain (data not shown). Taken together, these results confirm that *B. subtilis* MMG272 produces rhizocticin B and that the *rhi* gene cluster is responsible for its biosynthesis.

Proposed Rhizocticin Biosynthetic Pathway

On the basis of the amino acid sequence homology of Rhi proteins to enzymes with known activities and previous knowledge of phosphonate biosynthetic pathways, a proposed biosynthetic pathway for rhizocticins is shown in Figure 4. First, PEP is converted to PnPy by the action of the PEP mutase RhiH. PnPy then undergoes decarboxylation catalyzed by PnPy decarboxylase RhiE/RhiF to yield PnAA. These steps are common to the vast majority of known phosphonate antibiotic biosyntheses (Metcalf and van der Donk, 2009). The subsequent step is a novel transformation, an aldol reaction between PnAA and pyruvate (Py) catalyzed by the aldolase homolog RhiG. An alternative possibility is that the enolate of pyruvate is generated by decarboxylation of OAA (see below).

A minimum of two steps, dehydration and aminotransfer, are required to convert the putative RhiG product **I** to APPA. The aminotransferase RhiJ is likely responsible for the introduction of the amino group at C-2. It is less obvious how dehydration happens. It is possible that the aminotransferase RhiJ is also capable of catalyzing a PLP-dependent γ-elimination of water in tandem with aminotransfer, single-handedly converting **I** to APPA. Another possibility is activation of the hydroxyl leaving group via phosphorylation by the action of the kinase homolog RhiI. Elimination could then be achieved by a yet unknown activity of RhiI (e.g., via acid-base catalysis) or by the action of RhiJ. Alternatively, RhiG could be responsible for aldol addition followed by dehydration. Regardless of the order in which dehydration and aminotransfer happen (path "a" versus "b"), the APPA product can then be decorated at its N terminus with Arg and Val (or Leu/Ile) by the action of carboxylate-amine ligases. Two of these proteins, RhiC and RhiM, are encoded by the *rhi* cluster, suggesting that each of the peptide bonds is formed by the action of a dedicated ligase.

The timing of dehydration could also be later in the pathway. Namely, once intermediate **I** is converted by RhiJ to amino acid **III**, **III** may be incorporated by RhiC and RhiM into di- or tripeptide precursors **IV** of rhizocticins. In this case, the dehydration would commence on a peptide intermediate **IV**. In this scenario, no α-amino group would be available for RhiJ-catalyzed PLP-dependent chemistry and at least one another enzyme must be involved. This path ("c") is particularly appealing because it avoids the presence of toxic APPA as an intermediate.

The functions of the proteins RhiK, RhiL, and RhiN are unclear. Although unusual for secondary metabolite biosynthesis, the glutaredoxin homolog RhiK may be involved in maintaining a reduced active state for specific proteins of the pathway, and RhiL or RhiN or both may be involved in a dehydration sequence. Further studies are needed to clarify the functions of these proteins.

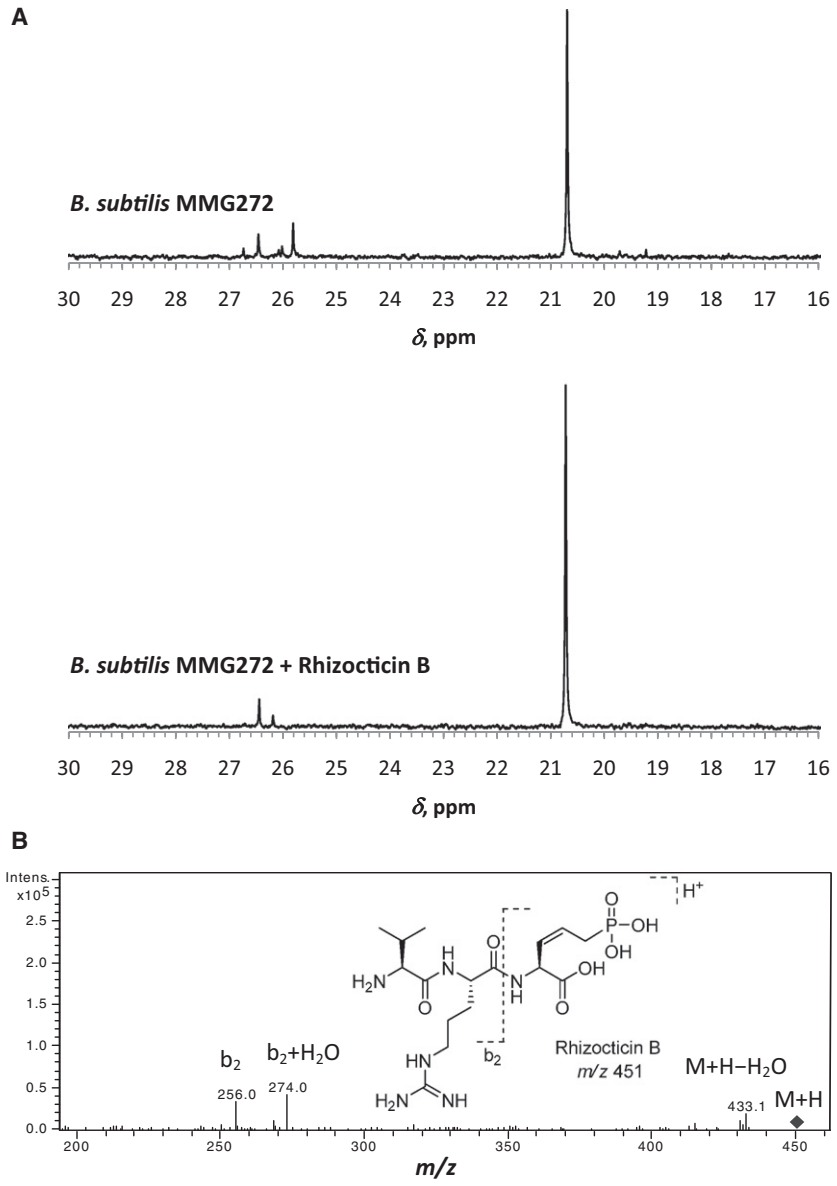

Figure 3. Analysis of rhizocticin B Production by *B. subtilis* MMG272

(A) ^{31}P NMR spectra of partially purified spent medium of *B. subtilis* MMG272 and of the same sample supplemented with rhizocticin B authentic standard. The concentrations of components in the sample *B. subtilis* MMG272 + rhizocticin B are the same as in the individual sample of *B. subtilis* MMG272. Both spectra were collected for 400 transients and adjusted to the same absolute vertical scale.

(B) LC-MS analysis of partially purified spent medium of *B. subtilis* MMG272. The fragmentation of the rhizocticin B parent ion is shown, and the peaks corresponding to the characteristic fragments are labeled.

Catalytic Activity of the PEP Mutase RhiH

The *rhiH* gene encoding putative PEP mutase was expressed in *E. coli* as a fusion protein with an N-terminal hexahistidine tag. Recombinant RhiH-N-His was purified to near homogeneity using metal affinity chromatography. The reversible reaction catalyzed by PEP mutase favors the formation of PEP (Seidel et al., 1988; Bowman et al., 1988). Subsequent decarboxylation of PnPy to PnAA catalyzed by PnPy decarboxylase provides the necessary driving force in many phosphonate pathways. Therefore, the enzymatic activity of RhiH-N-His was tested using a coupled assay with PnPy decarboxylase from *Bacteroides fragilis* (Zhang et al., 2003b) prepared as a C-terminally His-tagged protein (Ppd-Bf-His).

Assay conditions were based on published procedures (Zhang et al., 2003a; Blodgett et al., 2007) and are described in detail in the Supplemental Information. Briefly, the assay mixture containing PEP, catalytic TPP cofactor, and Mg^{2+} was incubated with RhiH-N-His and Ppd-Bf-His. The extent of the reaction was analyzed using ^{31}P NMR spectroscopy. Upon incubation, PEP (−0.2 ppm) was converted to PnAA, as demonstrated by the appearance of a new peak at 9.9 ppm in the ^{31}P NMR spectrum, consistent with the reported value (Blodgett et al., 2007). Upon prolonged storage, PnAA undergoes a nonenzymatic degradation, as attested by the appearance of a broad peak at 15.4 ppm in the ^{31}P NMR spectrum consistent with previously reported behavior (Zhang et al., 2003a).

RhiH-N-His, together with Ppd-Bf-His, were used for the enzymatic preparation of PnAA. Because of the labile nature of PnAA, the enzyme-free reaction mixture was used as a source of PnAA without further purification.

Investigation of RhiG Catalytic Activity

To obtain additional support for the biosynthetic proposal depicted in Figure 4, we set out to experimentally confirm the function of RhiG. Obtaining the product of RhiG via an enzymatic reaction would also provide the substrate for biochemical investigation of subsequent biosynthetic steps. RhiG was purified as a C-terminal fusion with a hexahistidine tag, RhiG-C-His (molecular weight, 38.7 kDa), using metal affinity chromatography. The purified protein contained no chromophore as attested by a UV-vis spectrum transparent above 300 nm. Native RhiG-C-His appears to be a homodimer (native molecular weight, 75 kDa) as determined by size-exclusion chromatography.

As seen for other class II aldolases, we expected that the activity of RhiG is dependent on a divalent metal cation, most likely Mg^{2+} or Mn^{2+}. Because the PnAA solution prepared with RhiH-N-His and Ppd-Bf-His already contains Mg^{2+}, no additional metals were supplied to the reaction. Incubation of a PnAA solution with pyruvate and RhiG-C-His did not produce new phosphonate compounds when examined by ^{31}P NMR spectroscopy. We then evaluated OAA as substrate for the aldol reaction with PnAA. Indeed, incubation of PnAA with OAA and

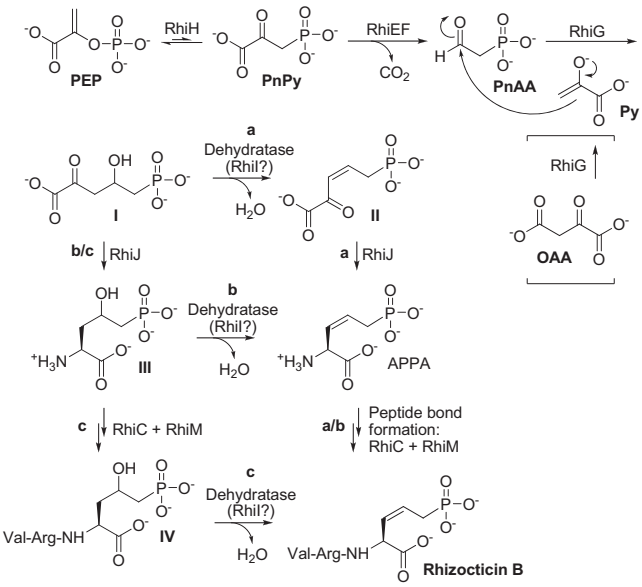

Figure 4. Proposed Pathways for the Biosynthesis of Rhizocticins

RhiG-C-His resulted in the formation of a new compound, denoted **Ia**, as demonstrated by the appearance of a new peak (19.8 ppm) in the ^{31}P NMR spectrum (Figure 5B). Approximately 80% of the PnAA was converted to **Ia**, as estimated by integration of the ^{31}P NMR signals. The product **Ia** was observed only when OAA and RhiG-C-His were both added to the assay. No new phosphonates were detected when 2-ketoglutaric acid was used in place of OAA. Interestingly, upon storage of the enzyme-free assay mixture, a slow conversion occurred of the phosphonate **Ia** to another phosphonate-containing compound (15.8 ppm), denoted **Ib**. Degradation of **Ia** and its highly polar nature complicated its purification by HPLC. Therefore, the structures of compounds **Ia** and **Ib** were determined using spectroscopic analyses of a crude assay mixture.

A comprehensive NMR analysis of the RhiG-C-His reaction mixtures prepared with unlabeled and ^{13}C-labeled PEP and OAA substrates (Supplemental Information and Figures S3 and S4) allowed for the unequivocal assignment of the structures **Ia** and **Ib** (Figure 5A). The structure of **Ia** was further supported by LC-MS analysis (Supplemental Information and Figure S5). The *trans* configuration of the double bond in **Ib**, and not a *cis* double bond as seen in APPA, suggests nonenzymatic formation of **Ib** with *anti*-elimination of water from **Ia** resulting in a *trans*-isomer. Therefore, the involvement of a specific enzyme (other than RhiG) is necessary for the dehydration during rhizocticin biosynthesis.

RhiG-C-His also catalyzes the formation of pyruvate from OAA in the absence of PnAA. This conversion was complete after incubation with RhiG-C-His at room temperature for 15 min, whereas only 13% of OAA was converted to pyruvate in the absence of enzyme (Supplemental Information).

Summary of the RhiG Reaction

RhiG catalyzes the formation of 2-keto-4-hydroxy-5-phosphonopentanoic acid from PnAA and OAA. Carbon dioxide is presumably a second product of this reaction. The requirement for divalent metal cation was not investigated at this point but is assumed on the basis of the studies of known class II aldolases. Clearly, if required, Mg^{2+} present in the assay was sufficient for successful conversion to **I**. OAA serves as a surrogate of pyruvate, and the corresponding three-carbon moiety is incorporated into the final product. We propose that OAA coordinates to a divalent metal cation (Mg^{2+} in our assay) via its 1-carboxylate and 2-ketone moieties and undergoes decarboxylation to produce the enolate form of pyruvate. The enolate is stabilized by the divalent cation acting as an electron sink. Subsequent attack of the enolate on the electrophilic carbonyl moiety of PnAA furnishes the carbon-carbon bond of **I** (Figure 6A).

The proposed RhiG mechanism draws from the homology of RhiG to 4-hydroxy-2-oxovalerate aldolase DmpG. Particularly, the residues comprising Mn^{2+} ligands in DmpG are also conserved in RhiG (Figure 6B) (Manjasetty et al., 2003). A crystal structure of DmpG contains either pyruvate (a product) or oxalate (a structural analog of pyruvate enolate) as an equatorial bidentate ligand to Mn^{2+} (Manjasetty et al., 2003). An analogous position could be occupied by OAA in RhiG as depicted in Figure 6A.

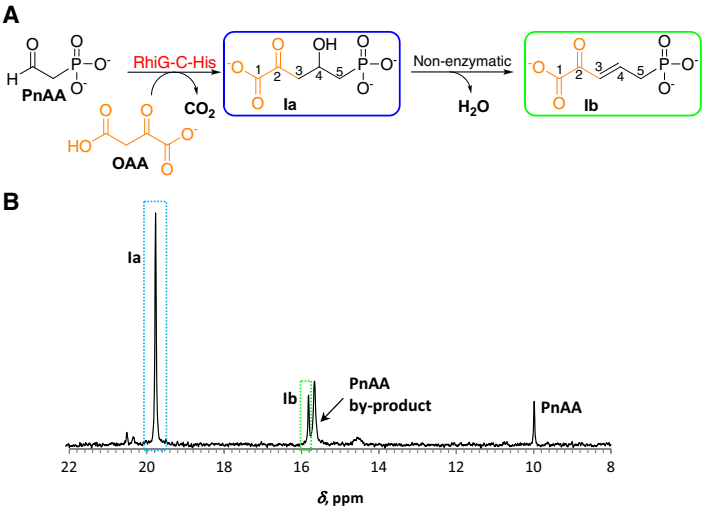

Figure 5. Reaction Catalyzed by RhiG-C-His

(A) Chemical reaction equation for the RhiG-C-His catalyzed process. (B) ^{31}P NMR spectrum of the RhiG-C-His assay with unlabeled substrates.

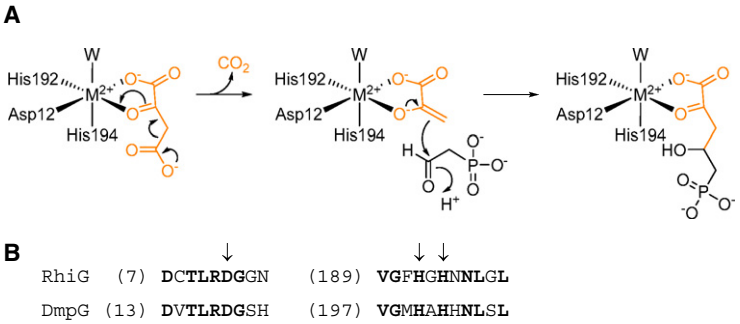

Figure 6. Proposed Mechanism for the RhiG-Catalyzed Transformation

Amino acid residues coordinating the divalent metal cation (panel A, RhiG numbering, W denotes water) are based on the alignment with the homolog DmpG shown in panel B (conserved residues are in bold, ligands to M^{2+} are labeled with arrows).

The first step in this mechanistic proposal, decarboxylation of OAA, is analogous to that catalyzed by macrophomate synthase from the fungus *Macrophoma commelinae* (Watanabe et al., 2000), (Ose et al., 2003). The pyruvate enolate generated by macrophomate synthase is stabilized by coordination to Mg^{2+} and carries out either a Diels-Alder or Michael-type aldol reaction, the specifics still being a matter of debate. Macrophomate synthase was recently reported to also possess promiscuous aldolase activity catalyzing an aldol reaction of OAA with aldehydes, analogous to the RhiG transformation (Serafimov et al., 2008). Interestingly, the amino acid sequence of RhiG has no homology to that of macrophomate synthase.

SIGNIFICANCE

Despite the demonstrated utility of phosphonates as therapeutics and agricultural chemicals, our knowledge of phosphonate biosynthetic pathways remains limited to a handful of examples (Metcalf and van der Donk, 2009). We report here the identification of the gene cluster responsible for the biosynthesis of rhizocticins in *B. subtilis* ATCC6633 and biochemical characterization of early transformations in the biosynthetic pathway. In addition to gaining valuable insight into the details of phosphonate biosynthesis, access to the pathway intermediate allows further investigation of the subsequent steps in the pathway and ultimately may provide a source of biologically active APPA or APPA-containing peptides.

The majority of currently known phosphonate biosynthetic pathways share PnAA as a common intermediate (Metcalf and van der Donk, 2009). The metabolic fate of PnAA is either transamination or reduction. Transamination produces 2-aminoethylphosphonate (AEP), which is incorporated into a variety of structural macromolecules, such as lipids and polysaccharides. Reduction, on the other hand, generates 2-hydroxyethylphosphonate (HEP) and leads to antibiotics such as fosfomycin, PTT, and dehydrophos. In this work, we discovered a third route by which phosphonate natural products are made from PnAA—through an aldol reaction with oxaloacetate. This type of transformation may prove to be a gateway to greater diversity of natural phosphonate compounds.

EXPERIMENTAL PROCEDURES

Materials

Chemical reagents used in this study were the products of Sigma-Aldrich (St. Louis, MO) or Thermo Fisher Scientific (Pittsburgh, PA) and were used without further purification. ^{13}C-labeled phosphoenolpyruvic acid potassium salt and aspartate were from Isotec of Sigma-Aldrich group. Media components were purchased from Thermo Fisher Scientific or VWR (West Chester, PA). Bacterial strains and PCR primers are listed in Tables S1 and S2, respectively.

Preparation of Rhizocticin Heterologous Producer *B. subtilis* MMG272

The spectinomycin cassette was incorporated into 2-11E fosmid (Supplemental Information) using λ Red mediated recombination (Datsenko and Wanner, 2000) with modifications as described below. A spectinomycin resistance cassette was amplified by PCR with primers Spec-red-fwd2 and Spec-red-rev2 using pAIN750 as a template. The primers were designed to contain 51 bp regions of homology to the sequences flanking the site of Spec insertion in fosmid 2-11E. The PCR product (Spec fragment, 1247 nt) was digested with DpnI and purified from an agarose gel. Electrocompetent *E. coli* MMG194 was transformed with pKD46, plated on LB agar containing 12 μg/mL chloramphenicol (Cm) and 100 μg/mL ampicillin (Amp), and grown at 30°C overnight. One of the transformants was picked and grown overnight at 30°C in LB-Cm, Amp. The culture was then diluted 100-fold into SOB medium containing Cm, Amp, and 2 mM arabinose (to induce λ recombinase) and grown to OD_{600} ~0.6 at 30°C. The cells were made electrocompetent by extensive washing with ice-cold 10% glycerol and were concentrated 100-fold. These cells (50 μl aliquot) were transformed with the PCR fragment (35 ng) via electroporation, recovered in SOC medium at 37°C for 2 hr, and plated on LB agar containing 7 μg/mL Cm and 100 μg/mL spectinomycin (Spec). Several colonies were inoculated into LB-Cm, Spec and grown overnight at 37°C. The fosmid DNA was isolated using QIAprep kit and analyzed by PCR amplification of the *rhiC*, *rhiM* genes and Spec fragment. The amplification of the DNA fragments of the desired size confirmed the incorporation of Spec into 2-11E and formation of fosmid 2-11E+Spec.

The fosmid DNA 2-11E+Spec was used to transform *E. coli* WM4489 to yield *E. coli* MMG273 strain. This strain was grown in the presence of 10 mM rhamnose to induce a high copy number for the fosmid 2-11E+Spec, and the fosmid DNA was reisolated. The 2-11E+Spec DNA was digested by restriction endonuclease NotI, purified by ethanol precipitation, and used to transform *B. subtilis* 168 following a published protocol (Henner, 1990). Recombinants were selected on LB agar plates containing 100 μg/mL Spec. The recombination was confirmed by culture PCR of selected recombinant strains as described above for verification of the fosmid 2-11E+Spec. One of the strains, *B. subtilis* MMG272, was chosen for rhizocticin production analysis as described below.

Rhizocticin B Production in *B. subtilis* MMG272 and Analysis by ^{31}P NMR Spectroscopy and LC-MS

The heterologous producer *B. subtilis* MMG272 was grown for metabolite production, as described for *B. subtilis* ATCC6633 (Supplemental Information), with several exceptions. Spectinomycin was added to all of the media at 100 μg/mL. Additionally, PL medium was supplemented with tryptophan at 50 μg/mL, and the fermentation culture volume was 2 L. The cell-free supernatant was taken through the same purification steps through Biogel P2 fractionation as described for rhizocoticin purification (Supplemental Information). The P2 fractions corresponding to the rhizocticin B elution volume were analyzed by ^{31}P NMR spectroscopy and compared to an authentic standard. Several phosphonates with chemical shifts in the range 17–27 ppm were detected;

fractions eluted from the column with 90–100 ml of water (B7-8) contained a major phosphonate with a chemical shift of 20.7 ppm. The NMR sample of B7-8 was supplemented with 8 mM rhizocticin B and reanalyzed by ^{31}P NMR spectroscopy. Sample B7-8 was analyzed by LC-MS as described for rhizocticin B analysis (Supplemental Information), and its retention time and fragmentation pattern were consistent with the presence of rhizocticin B (Figure 3B).

RhiG Activity Assays

A stock of 100 mM oxaloacetic acid was freshly prepared in 100 mM sodium cacodylate buffer (pH 7.5). It was added to the PnAA sample (Supplemental Information) to a final OAA concentration of 12 mM. The reaction was initiated by the addition of RhiG-C-His (45 μM, see the Supplemental Information for the details of the protein purification) and the assay mixture was incubated at 30°C for 1 hr. A precipitate that formed during incubation was removed by centrifugation, and soluble proteins were removed by filtration through a Microcon YM-30 unit. We found that adding OAA and RhiG without prior removal of RhiH-N-His and Ppd-Bf-His, or even simultaneously with PnAA formation, reduced the amount of the PnAA degradation product formed. Therefore, the samples intended for extensive NMR characterization were prepared in this manner to reduce the processing time. The Microcon units were sequentially rinsed with 0.1 M sodium hydroxide, water, and finally reaction buffer prior to use to eliminate trace amounts of glycerol because it produced ^{1}H NMR signals in the region of interest. The enzymatic preparation of ^{13}C-labeled compounds and the spectroscopic characterization of compounds **Ia**, **Ib**, **Ia**′,**Ia**″ and **Ib**′ are described in the Supplemental Information.

ACCESSION NUMBER

The sequence of the insert in fosmid 2-11E containing rhizocticin biosynthetic gene cluster has been deposited in GenBank under accession number FJ935779.

SUPPLEMENTAL INFORMATION

Supplemental Information includes five figures, two tables, and Experimental Procedures. It can be found with this article online at doi:10.1016/j.chembiol.2009.11.017.

ACKNOWLEDGMENTS

We thank Feng Lin (Keck NMR laboratory, UIUC) for assistance with advanced NMR experiments, Lucas Li (Biotechnology Center, UIUC) for performing LC-MS analysis, and Nurul Zulkepli for help in preparation of pRhiG-C-His. This work was supported by the National Institutes of Health (GM PO1 GM077596). Its contents are solely the responsibility of the authors and do not necessarily represent the official views of the NIGMS or NIH.

Received: October 19, 2009
Revised: November 23, 2009
Accepted: November 30, 2009
Published: January 28, 2010

REFERENCES

Altschul, S.F., Gish, W., Miller, W., Myers, E.W., and Lipman, D.J. (1990). Basic local alignment search tool. J. Mol. Biol. *215*, 403–410.

Artymiuk, P.J., Poirrette, A.R., Rice, D.W., and Willett, P. (1996). Biotin carboxylase comes into the fold. Nat. Struct. Biol. *3*, 128–132.

Aziz, R.K., Bartels, D., Best, A.A., DeJongh, M., Disz, T., Edwards, R.A., Formsma, K., Gerdes, S., Glass, E.M., Kubal, M., et al. (2008). The RAST Server: rapid annotations using subsystems technology. BMC Genomics *9*, 75.

Blodgett, J.A., Zhang, J.K., and Metcalf, W.W. (2005). Molecular cloning, sequence analysis, and heterologous expression of the phosphinothricin tripeptide biosynthetic gene cluster from *Streptomyces viridochromogenes* DSM 40736. Antimicrob. Agents Chemother. *49*, 230–240.

Blodgett, J.A., Thomas, P.M., Li, G., Velasquez, J.E., van der Donk, W.A., Kelleher, N.L., and Metcalf, W.W. (2007). Unusual transformations in the biosynthesis of the antibiotic phosphinothricin tripeptide. Nat. Chem. Biol. *3*, 480–485.

Bowman, E., McQueney, M., Barry, R.J., and Dunaway-Mariano, D. (1988). Catalysis and thermodynamics of the phosphoenolpyruvate/phosphonopyruvate rearrangement: entry into the phosphonate class of naturally occurring organophosphorus compounds. J. Am. Chem. Soc. *110*, 5575–5576.

Cicchillo, R.M., Zhang, H., Blodgett, J.A., Whitteck, J.T., Li, G., Nair, S.K., van der Donk, W.A., and Metcalf, W.W. (2009). An unusual carbon-carbon bond cleavage reaction during phosphinothricin biosynthesis. Nature *459*, 871–874.

Datsenko, K.A., and Wanner, B.L. (2000). One-step inactivation of chromosomal genes in *Escherichia coli* K-12 using PCR products. Proc. Natl. Acad. Sci. USA *97*, 6640–6645.

Diddens, H., Dorgerloh, M., and Zahner, H. (1979). Metabolic products of microorganisms. 176. On the transport of small peptide antibiotics in bacteria. J. Antibiot. (Tokyo) *32*, 87–90.

Eliot, A.C., and Kirsch, J.F. (2004). Pyridoxal phosphate enzymes: mechanistic, structural, and evolutionary considerations. Annu. Rev. Biochem. *73*, 383–415.

Eliot, A.C., Griffin, B.M., Thomas, P.M., Johannes, T.W., Kelleher, N.L., Zhao, H., and Metcalf, W.W. (2008). Cloning, expression, and biochemical characterization of *Streptomyces rubellomurinus* genes required for biosynthesis of antimalarial compound FR900098. Chem. Biol. *15*, 765–770.

Fan, C., Moews, P.C., Walsh, C.T., and Knox, J.R. (1994). Vancomycin resistance: structure of D-alanine:D-alanine ligase at 2.3 A resolution. Science *266*, 439–443.

Fan, C., Moews, P.C., Shi, Y., Walsh, C.T., and Knox, J.R. (1995). A common fold for peptide synthetases cleaving ATP to ADP: glutathione synthetase and D-alanine:D-alanine ligase of *Escherichia coli*. Proc. Natl. Acad. Sci. USA *92*, 1172–1176.

Galperin, M.Y., and Koonin, E.V. (1997). A diverse superfamily of enzymes with ATP-dependent carboxylate-amine/thiol ligase activity. Protein Sci. *6*, 2639–2643.

Gonzalez-Pastor, J.E., Hobbs, E.C., and Losick, R. (2003). Cannibalism by sporulating bacteria. Science *301*, 510–513.

Graupner, M., Xu, H., and White, R.H. (2000). Identification of the gene encoding sulfopyruvate decarboxylase, an enzyme involved in biosynthesis of coenzyme M. J. Bacteriol. *182*, 4862–4867.

Helgadottir, S., Rosas-Sandoval, G., Soll, D., and Graham, D.E. (2007). Biosynthesis of phosphoserine in the *Methanococcales*. J. Bacteriol. *189*, 575–582.

Henner, D.J. (1990). Inducible expression of regulatory genes in *Bacillus subtilis*. Methods Enzymol. *185*, 223–228.

Hidaka, T., Goda, M., Kuzuyama, T., Takei, N., Hidaka, M., and Seto, H. (1995). Cloning and nucleotide sequence of fosfomycin biosynthetic genes of *Streptomyces wedmorensis*. Mol. Gen. Genet. *249*, 274–280.

Higgins, L.J., Yan, F., Liu, P., Liu, H.W., and Drennan, C.L. (2005). Structural insight into antibiotic fosfomycin biosynthesis by a mononuclear iron enzyme. Nature *437*, 838–844.

Kelley, L.A., and Sternberg, M.J. (2009). Protein structure prediction on the Web: a case study using the Phyre server. Nat. Protoc. *4*, 363–371.

Kino, K., Nakazawa, Y., and Yagasaki, M. (2008a). Dipeptide synthesis by L-amino acid ligase from *Ralstonia solanacearum*. Biochem. Biophys. Res. Commun. *371*, 536–540.

Kino, K., Noguchi, A., Nakazawa, Y., and Yagasaki, M. (2008b). A novel L-amino acid ligase from *Bacillus licheniformis*. J. Biosci. Bioeng. *106*, 313–315.

Kino, K., Kotanaka, Y., Arai, T., and Yagasaki, M. (2009). A novel L-amino acid ligase from *Bacillus subtilis* NBRC3134, a microorganism producing peptide-antibiotic rhizocticin. Biosci. Biotechnol. Biochem. *73*, 901–907.

Koonin, E.V. (1994). Conserved sequence pattern in a wide variety of phosphoesterases. Protein Sci. *3*, 356–358.

Kugler, M., Loeffler, W., Rapp, C., Kern, A., and Jung, G. (1990). Rhizocticin A, an antifungal phosphono-oligopeptide of *Bacillus subtilis* ATCC6633: biological properties. Arch. Microbiol. *153*, 276–281.

Kunst, F., Ogasawara, N., Moszer, I., Albertini, A.M., Alloni, G., Azevedo, V., Bertero, M.G., Bessieres, P., Bolotin, A., Borchert, S., et al. (1997). The complete genome sequence of the gram-positive bacterium *Bacillus subtilis*. Nature *390*, 249–256.

Laber, B., Lindell, S.D., and Pohlenz, H.D. (1994). Inactivation of *Escherichia coli* threonine synthase by DL-*Z*-2-amino-5-phosphono-3-pentenoic acid. Arch. Microbiol. *161*, 400–403.

Lauer, B., Russwurm, R., Schwarz, W., Kalmanczhelyi, A., Bruntner, C., Rosemeier, A., and Bormann, C. (2001). Molecular characterization of co-transcribed genes from *Streptomyces tendae* Tu901 involved in the biosynthesis of the peptidyl moiety and assembly of the peptidyl nucleoside antibiotic nikkomycin. Mol. Gen. Genet. *264*, 662–673.

Li, Y., Zeng, H., and Tan, H. (2004). Cloning, function, and expression of *sanS*: a gene essential for nikkomycin biosynthesis of *Streptomyces ansochromogenes*. Curr. Microbiol. *49*, 128–132.

Maddocks, S.E., and Oyston, P.C. (2008). Structure and function of the LysR-type transcriptional regulator (LTTR) family proteins. Microbiology *154*, 3609–3623.

Manjasetty, B.A., Powlowski, J., and Vrielink, A. (2003). Crystal structure of a bifunctional aldolase-dehydrogenase: sequestering a reactive and volatile intermediate. Proc. Natl. Acad. Sci. USA *100*, 6992–6997.

Martin-Verstraete, I., Deutscher, J., and Galinier, A. (1999). Phosphorylation of HPr and Crh by HprK, early steps in the catabolite repression signalling pathway for the *Bacillus subtilis* levanase operon. J. Bacteriol. *181*, 2966–2969.

Mehta, P.K., Hale, T.I., and Christen, P. (1993). Aminotransferases: demonstration of homology and division into evolutionary subgroups. Eur. J. Biochem. *214*, 549–561.

Metcalf, W.W., and van der Donk, W.A. (2009). Biosynthesis of phosphonic and phosphinic acid natural products. Annu. Rev. Biochem. *78*, 65–94.

Michener, H.D., and Snell, N. (1949). Two antifungal substances from *Bacillus subtilis* cultures. Arch. Biochem. *22*, 208–214.

Morett, E., Saab-Rincon, G., Olvera, L., Olvera, M., Flores, H., and Grande, R. (2008). Sensitive genome-wide screen for low secondary enzymatic activities: the YjbQ family shows thiamin phosphate synthase activity. J. Mol. Biol. *376*, 839–853.

Ose, T., Watanabe, K., Mie, T., Honma, M., Watanabe, H., Yao, M., Oikawa, H., and Tanaka, I. (2003). Insight into a natural Diels-Alder reaction from the structure of macrophomate synthase. Nature *422*, 185–189.

Pan, J.L., and Bardwell, J.C. (2006). The origami of thioredoxin-like folds. Protein Sci. *15*, 2217–2227.

Park, B.K., Hirota, A., and Sakai, H. (1977a). Structure of plumbemycin-A and plumbemycin-B, antagonists of L-threonine from *Streptomyces plumbeus*. Agric. Biol. Chem. *41*, 573–579.

Park, B.K., Hirota, A., and Sakai, H. (1977b). Studies on new antimetabolite N-1409. Agric. Biol. Chem. *41*, 161–167.

Peapus, D.H., Chiu, H.J., Campobasso, N., Reddick, J.J., Begley, T.P., and Ealick, S.E. (2001). Structural characterization of the enzyme-substrate, enzyme-intermediate, and enzyme-product complexes of thiamin phosphate synthase. Biochemistry *40*, 10103–10114.

Platt, A., Shingler, V., Taylor, S.C., and Williams, P.A. (1995). The 4-hydroxy-2-oxovalerate aldolase and acetaldehyde dehydrogenase (acylating) encoded by the *nahM* and *nahO* genes of the naphthalene catabolic plasmid pWW60-22 provide further evidence of conservation of meta-cleavage pathway gene sequences. Microbiology *141*, 2223–2233.

Rapp, C., Jung, G., Kugler, M., and Loeffler, W. (1988). Rhizocticins—new phosphono-oligopeptides with antifungal activity. Liebigs Ann. Chem., 655–661.

Schell, M.A. (1993). Molecular biology of the LysR family of transcriptional regulators. Annu. Rev. Microbiol. *47*, 597–626.

Seidel, H.M., Freeman, S., Seto, H., and Knowles, J.R. (1988). Phosphonate biosynthesis: isolation of the enzyme responsible for the formation of a carbon-phosphorus bond. Nature *335*, 457–458.

Serafimov, J.M., Gillingham, D., Kuster, S., and Hilvert, D. (2008). The putative Diels-Alderase macrophomate synthase is an efficient aldolase. J. Am. Chem. Soc. *130*, 7798–7799.

Tabata, K., Ikeda, H., and Hashimoto, S. (2005). *ywfE* in *Bacillus subtilis* codes for a novel enzyme, L-amino acid ligase. J. Bacteriol. *187*, 5195–5202.

Waldrop, G.L., Rayment, I., and Holden, H.M. (1994). Three-dimensional structure of the biotin carboxylase subunit of acetyl-CoA carboxylase. Biochemistry *33*, 10249–10256.

Watanabe, K., Mie, T., Ichihara, A., Oikawa, H., and Honma, M. (2000). Detailed reaction mechanism of macrophomate synthase: extraordinary enzyme catalyzing five-step transformation from 2-pyrones to benzoates. J. Biol. Chem. *275*, 38393–38401.

Woodyer, R.D., Shao, Z., Thomas, P.M., Kelleher, N.L., Blodgett, J.A., Metcalf, W.W., van der Donk, W.A., and Zhao, H. (2006). Heterologous production of fosfomycin and identification of the minimal biosynthetic gene cluster. Chem. Biol. *13*, 1171–1182.

Yamaguchi, H., Kato, H., Hata, Y., Nishioka, T., Kimura, A., Oda, J., and Katsube, Y. (1993). Three-dimensional structure of the glutathione synthetase from *Escherichia coli* B at 2.0 A resolution. J. Mol. Biol. *229*, 1083–1100.

Zawadzke, L.E., Bugg, T.D., and Walsh, C.T. (1991). Existence of two D-alanine:D-alanine ligases in *Escherichia coli*: cloning and sequencing of the *ddlA* gene and purification and characterization of the DdlA and DdlB enzymes. Biochemistry *30*, 1673–1682.

Zhang, G., Allen, K.N., and Dunaway-Mariano, D. (2003a). Enzymatic synthesis of radiolabeled phosphonoacetaldehyde. Anal. Biochem. *322*, 233–237.

Zhang, G., Dai, J., Lu, Z., and Dunaway-Mariano, D. (2003b). The phosphonopyruvate decarboxylase from *Bacteroides fragilis*. J. Biol. Chem. *278*, 41302–41308.